Survey of the Ridracoli Dam: UAV–based photogrammetry and traditional topographic techniques in the inspection of vertical structures

Giulia Buffi , Piergiorgio Manciola, Silvia Grassi, Marco Barberini & Andrea Gambi

Published online: 24 Aug 2017.

Submit your article to this journal

Article views: 73

View related articles

View Crossmark data

Taylor & Francis
Taylor & Francis Group

Survey of the Ridracoli Dam: UAV–based photogrammetry and traditional topographic techniques in the inspection of vertical structures

Giulia Buffi [ID][a], Piergiorgio Manciola[a], Silvia Grassi[b], Marco Barberini[c] and Andrea Gambi[d]

[a]University of Perugia, Via Goffredo Duranti, Perugia, Italy; [b]Studio Grassi, Via Luigi Salvatorelli, Perugia, Italy; [c]Italdron S.p.A., Via Faentina, Ravenna, Italy; [d]Romagna Acque Società delle Fonti S.p.A., Piazza del Lavoro, Forlì, Italy

ABSTRACT

The inspection of strategic works such as dams is of vital importance both for their maintenance and for the safety of downstream populations. The reduced accessibility, both for uptake needs and for their strategic nature, and the large time needed for an inspection by traditional method do not facilitate the investigation of this type of structures. The new unmanned aerial vehicle (UAV) technology, equipped with high-performance cameras, allows for rapid photographic coverage of the whole dam system. Apart from the placement on the structure of a high number of markers, the correct geo-referencing and validation of the model also requires an important terrestrial topographic campaign by total station, Global Positioning System and laser scanner. Punctual, linear and surface analysis shows the high accuracy of the drone acquiring technique. The product is suitable for a detailed survey of the conservation status of the materials and the complete metric reconstruction of the dam system and the adjacent land. The present work explains firstly a UAV acquisition and then the first dense point cloud validation procedure of a concrete arch gravity dam. The Ridracoli dam is the object of the survey, located in the village of Santa Sofia in central Italy.

Introduction

The safety and efficient maintenance of dams are primary aspects in the management of such strategic works (Tang and Yen 1991). Indeed, the failure of a dam can have tragic consequences, as testified by numerous dam break cases that occurred in the past (e.g. Zech and Soares-Frazão 2007; Froelich 2008; Biscarini et al. 2010; Biscarini et al. 2016; Kim and Sanders 2016). The need to combine, ever more effectively, the security with the containment of maintenance costs directly linked to the service life of the structure, requires innovative approaches beside traditional methods. Dams are built for several purposes, such as water supply, flood control, irrigation, navigation and hydropower generation. Dams are often the basis of multipurpose projects (Tortajada 2014; International Commission on Large Dams 2016). In Italy, there are 541 large dams, with an average life of over 50 years, which may extend to 70 years if the analysis is limited to the Alps (Marcello and Fornari 2012). Managers of restraint structures must ensure dam maintenance through frequent and continual activities, as well as fulfilling regulatory activities on the basis of information provided by institutional bodies (Casadei and Manciola 1995; DM Infrastrutture 14 gennaio 2008).

CONTACT Giulia Buffi ✉ giulia.buffi@unipg.it

The reduced accessibility of dams, both for uptake needs and for their strategic nature, and the large time needed for an inspection by traditional method do not facilitate direct visual inspection. Therefore, the use of unmanned aerial vehicle (UAV) is more suitable (Colomina and Molina 2014; Ellenberg, Branco et al. 2014; Ellenberg et al. 2014; Vetrivel et al. 2015). The use of UAVs is spreading to the safe inspection of sections of infrastructure that would otherwise not be directly accessible, except with expensive and dangerous procedures such as climbers. The state of conservation of the materials can be monitored (Salvini et al. 2016) in order to guaranty a proactive maintenance of the structure. Moreover, in most cases, the project geometry of ancillary works such as spillways is not available. Real shape modelling of these elements allows the spillway capacity correct evaluation, as well as the hydraulic profile of overflow. Some works deal with the three-dimensional (3D) modelling of flows such as Olsen and Kjellesvig (2010) and Biscarini et al. (2013).

UAV techniques are employed in surveys and metrical reconstruction in other fields, such as vegetation analysis (Venturi et al. 2016), coastal areas (Gonçalvesa and Henriques 2015), agriculture enhancement (Ouédraogo et al. 2014) and the inspection of the natural environment (Mancini et al. 2013), historical buildings (Achille et al. 2015; Hallermann et al. 2015; Dominici et al. 2016), bridges and viaducts (Gillins et al. 2016; Hallermann and Morgenthal 2016) and large-scale structures (e.g. retaining walls; Hallermann et al. 2014); civil buildings, chimneys and torches. Not ever in the mentioned works, a study on the accuracy and precision of the survey was done, comparing the UAV technique with the traditional ones such as total station (TS), Global Positioning System (GPS) station and laser scanner.

Moreover, the use of UAV equipment on dams is rare and at an early stage (e.g. Naumann et al. 2013). This paper presents the first 3D geometric reconstruction by UAV of a concrete arch gravity dam. The present work aims to provide an operative procedure for UAV survey operations and for the dense point cloud validation of masonry dams.

From the huge UAV photographic set, it is possible to obtain qualitative information, with the aim of recognizing the condition of the materials, as well as quantitative information. The 'Structure from Motion' (SfM) technique allows for the reconstruction of 3D objects from two-dimensional (2D) images (Ullman 1979; Irschara et al. 2009; Turner et al. 2012; Teza et al. 2016) in order to create a 3D model of the acquired structure (Püschel et al. 2008; Bolognesi et al. 2015). An extensive topographical survey, by TS, GPS and laser scanner (Bolognesi et al. 2014), is necessary to geo-reference and validate the UAV dense point cloud.

The paper is organized as follows. First, the case study of the Ridracoli dam is presented. The next section describes the integrated survey system tools (i.e. TS, terrestrial laser scanner (TLS), GPS and UAV). Second, the marker placement, the UAV survey and the UAV restitution are presented. This is followed by a description of the traditional topographic techniques and a punctual, linear and surface analysis to validate the global accuracy of the UAV dense point cloud. Finally, the results and conclusions are presented, which demonstrate the efficiency and effectiveness of the UAV technique in surveying dams.

Case study: the Ridracoli dam

The Ridracoli dam, managed by Romagna Acque Società delle Fonti S.p.A., is located in the village of Santa Sofia in the province of Forlì-Cesena, Emilia Romagna, Italy (Figure 1(a)). The primary use of the reservoir is to supply drinking water through the regulation of the flow of the Bidente river during the year (Figure 1(b)). The dam supplies the water needs of 48 municipalities in the provinces of Forlì-Cesena, Ravenna and Rimini and, since 1989, of Republic of San Marino (Alpina S.p.A., Consorzio Acque Forlì Ravenna 1985; Consorzio Acque per le Province di Forlì e Cesena 1991). The secondary function is the production of hydroelectricity for the surrounding area. The Ridracoli dam is a simple concrete arch gravity dam, 103.5 m high, with a crest 432 m long. The dam body is a double-curved structure, symmetrical with respect to the main section, resting on a foundation base that extends all around the perimeter of the abutments. The upstream and downstream facings, following specific analytical laws, give progressively increasing thickness to the arches along the
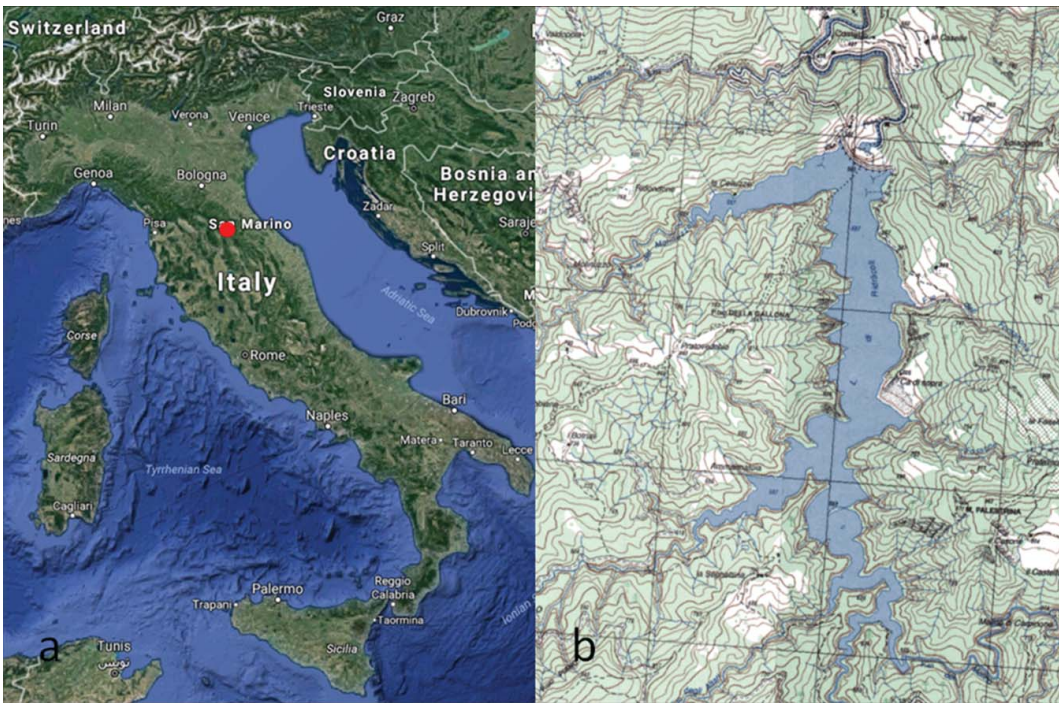
Figure 1. (a) Geographical collocation of the Ridracoli Dam (point) scale 1:200Km; (b) The lake created by the presence of the dam, scale 1:500 m (National Institute of Geophysics and Volcanology 2016).

horizontal sections, from the middle to the sides and along the vertical section from the top to the base, in line with the arch gravity construction type. The dam body is composed of 27 independent ashlars to ensure the deformation of the structure due to the increase of the hydrostatic level and other factors, such as the temperature, and to avoid the structure cracking.

System of integrated survey

This paper presents a survey of the Ridracoli Dam. This is a technological comparison between traditional topographic instruments and unconventional photogrammetry conducted by UAV. The topographic instruments used include TS (TS30 Leica-Geosystems), GPS Satellite Station (1230 Leica Leica-Geosystems) and laser scanner (Z+F 5010 ZoellerFroelich). The drone used is a four propeller HIGHONE 4HSEPRO, with an autonomy of 18–30 minutes and a Gimbal system with SONY Alpha 7R, 36.4 Mpix Full frame camera. Video images were acquired with a LUMIX GH4 Full Frame camera (FullHD video 1920 × 1080 29fps). Flight operations were performed in manual mode and image-shooting operations were followed by a second flight operator who was able to assess the entity of overlapping frames. The integrated survey system makes it possible to validate and geo-reference the model. In this way, topographic instruments act as a support for the drone and validate the survey.

Marker placement

To geo-reference the images shot during the UAV survey, in addition to natural points, it is necessary to place a proper number of markers on the dam and the surrounding areas (Figure 2). Natural points, to be considered as reference points, have to be fixed points, well visible and representative of the structure geometry such as curvature changes or vertices. Have been chosen 62 natural points. It was not possible to consider only natural points because the structure is mostly vertical and monochrome. A total of 226 markers of 40 × 40 cm in size were stably applied with the aid of
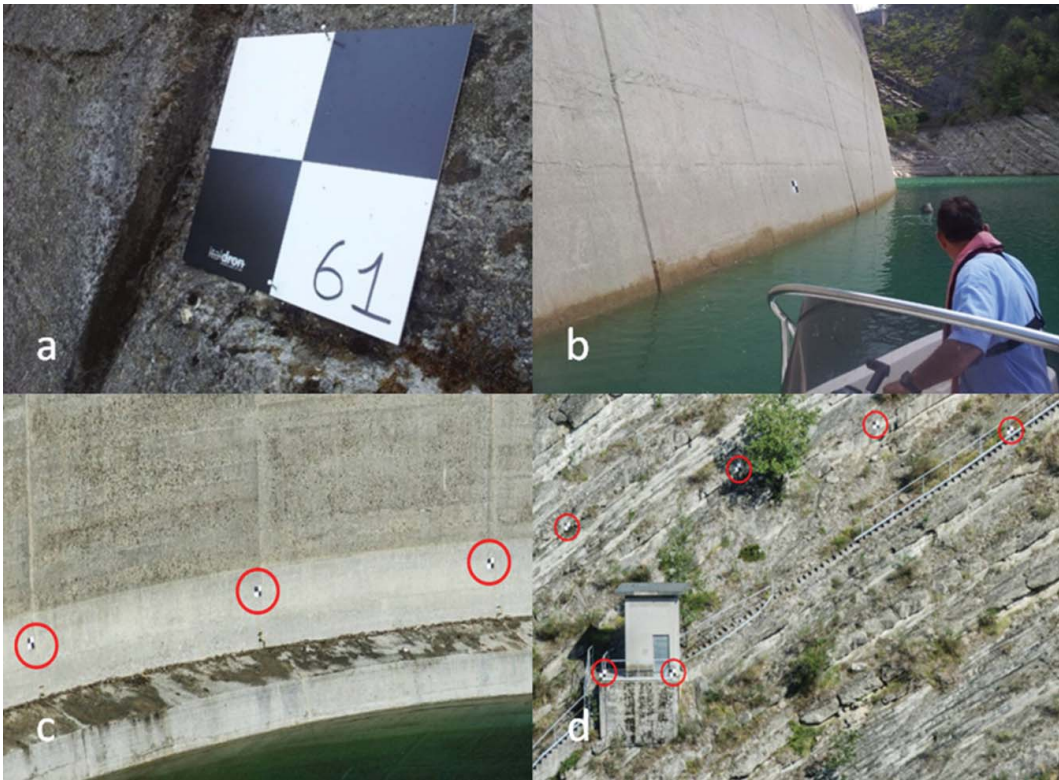
Figure 2. (a) Marker applied near a joint; (b) Marker application on the upstream face; (c) Marker application on the downstream face near the foundation base; (d) Marker application on an area located on the left side.

non-invasive fastening and simple removal techniques. The placement followed criteria of uniformity in distribution and visibility. Markers were placed on points identified as significant for the following finite element (FE) modelling. The markers were placed on the dam crest, on the parapet walls on either side of the roadway on the crest, on the adjacent portions of soil, on the step of the foundation base, on the stilling basin and on the upstream facing dam. Markers were placed at the hydrostatic level at the time of operations using a boat. The marker application operations employed three two-man teams for three days. In literature, there are no indications regarding a method which optimizes the distribution of markers in the case of a vertical structure survey; there are only some applications on extended horizontal surfaces (Barry and Coakley 2013; Tahar 2013; Skarlatos et al. 2013) or related to traditional topographic techniques such as laser scanner (Wujanz et al. 2016). Moreover, new research topic may be opened up with the application to this field of a statistical measurement such as informative entropy, seen as a measure of information associated with the observed data (e.g. Ridolfi et al. 2012; Alfonso et al. 2014; Ridolfi et al. 2014). The concept of entropy was introduced by Shannon (1948) and then applied in hydrology by Amorocho and Espildora (1973) due to its robustness. A further development of this work will focus on the investigation of optimal marker placement in terms of numbers and configurations (Ridolfi et al. 2017).

The flight and survey restitution by UAV – photogrammetric modelling

UAV flight operations were concentrated in a single day and aimed to cover with photographic frames the downstream facing dam, the upstream facing dam up to the hydrostatic level, the crest, the stilling basin, the right and left sides, the picnic area, the guardhouse and part of the surrounding land. Nineteen flights lasting 15 min/flight were performed, providing a total of 4600 frames at 36

megapixel resolution. The shooting operations were performed remotely by a second flight attendant, who evaluated the entity of overlapping frames. The distance of the UAV from the dam surfaces was around 15–25 m. In some areas, in fact, such as the downstream face, a flight at close range would be dangerous because of the warm ascending air flows due to the temperature difference between the bottom and the top of the structure. Moreover, these air updrafts and the complexity of the structure geometry did not allow an autopilot survey and manual flights have been performed. The post-processing of the acquired data was the most time-consuming procedure. The high resolution frames at 7360 × 4912 pixels have been divided in subareas, downstream and upstream faces, crowing of the dam, left (warden house and recreation area) and right sides, stilling basin and galleries in order to share the computational cost of the creation of the whole dense point cloud model. The build of every partitioned model employed about five days, including the frames loading and the ground control points (GCPs) picking, using medium-high performance hardware (Intel® Core™ i7 processor, 32 GB RAM, Nvidia® GeForce GTX graphics). The procedure took 45 working days plus the time required for assembling, overlapping and refining the dense point cloud parts that employed other 15 working days.

The 3D model was realized through the SfM technique (Ullman 1979). This technique allows for the reconstruction of the geometry of objects through the automatic collimation of points from a series of images.

The reconstruction of the dense point cloud was made using the SfM processing Cloud Compare® software for subsequent stages. First, the 36 megapixel images were analysed and geo-referenced using marker coordinates. Second, the frames were aligned and a cloud of low-density points was created; following this, another point cloud with a higher density was produced. On this high-density model, a 3D textured mesh was applied (Figure 3).


Figure 3. Texturized 3D mesh of the road way on the dam crest.

Conventional GPS and total station surveying

Two topographical networks were defined by TS. A primary network was identified, made up of four locations named BS, SS, DS and BD (Figure 4). The four points coincide with the pillars currently used to periodically monitor the dam. A secondary network was also created consisting of materialized points with nails driven into the ground, and this was connected to the primary network through topographic measurements. The primary and secondary networks detected a total of 417 points of the structure and the surrounding land, including markers and natural points. To obtain temporally homogeneous data, the topographic acquisition from TS and the frames acquired with the UAV technique were carried out simultaneously. The four vertices of the primary network were marked with GPS instrumentation and the obtained coordinates were converted into the Gauss–Boaga cartographic system and z-coordinates to properly geo-reference the entire model. For the transformation, the cartographic grid 107,606.gk2 (Verto 3 K), provided by the Military Geographical Institute (IGM) with reference to the vertices 107,606 Santa Sofia (Poggio la Guardia), located a few hundred meters from the top of the dam, was employed.

The coordinates of the measured points have a standard deviation lower than 1.0 cm in the three components east, north and height, and 0.7 cm on average. The coordinates have a small dispersion around their mean values (Table 1). It is interesting to note that the standard deviation values confirm the suitability of these 417 points for use in the geo-referencing of UAV frames and in the validation of the same model.
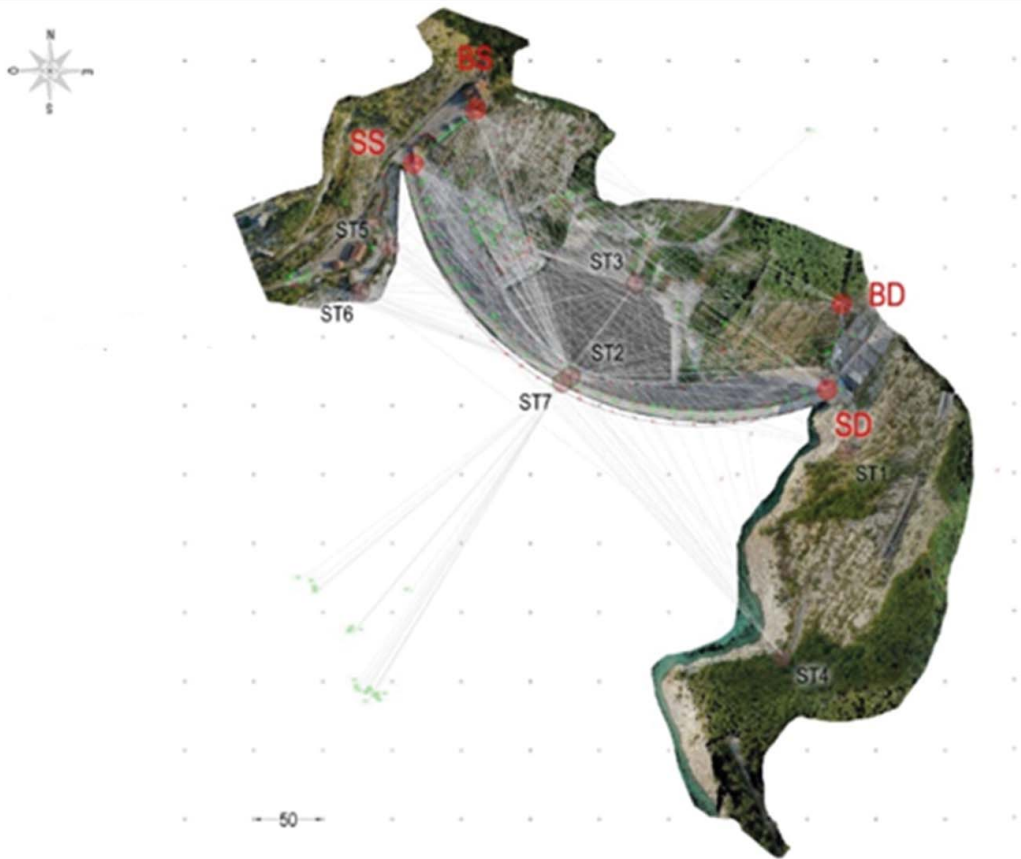
Figure 4. Topographic networks: a first network is composed of the four vertices (i.e. SS, BS, SD and BD) and a second network is composed of 11 other bases by which a total 417 points made of markers and natural points were acquired by the total station.

Table 1. Standard deviation of the 417 point coordinates detected by total station. The low σ values show the limited dispersion of the acquired coordinates along the three components.

	Standard deviations		
Total station	East (m)	North (m)	Altitude (m)
Maximum values	0.010	0.010	0.008
Medium values	0.006	0.007	0.004

Laser scanner surveying

To verify the acquisitions made by the drone, a laser scanner survey was performed. The resulting scans were compared with drone analysis, in analogy to the work performed by Andrews et al. (2013) for a historic building. Most surveys of existing structures employ only laser scanner analysis, as performed on a historical tower by Achille et al. (2015).

The dam model obtained by the laser scanner survey involved nine acquisition workstations in order to acquire most of the surface area of the structure. Figure 5 shows the basis of the acquisition and each corresponding analysed area. A selection of the aforementioned markers was used to geo-reference the scans. The decision to use part of the same markers of the photogrammetric model was made to ensure the perfect match between the two image data sets. To record each individual scan, 53 markers were employed, whose topographic coordinates, acquired by TS, are characterized by an average standard deviation of less than 1 cm (Table 1). Table 2 shows the results of recording scans. The residuals between the marker coordinates acquired by TS and laser scanner have average values in all cases less than 1 cm, and the correspondent standard deviations do not exceed the value of 5 mm. It is interesting to note that these values are lower than both the accuracies and the standard deviations of the topographic coordinates acquired by TS. Therefore, the scans are suitable to
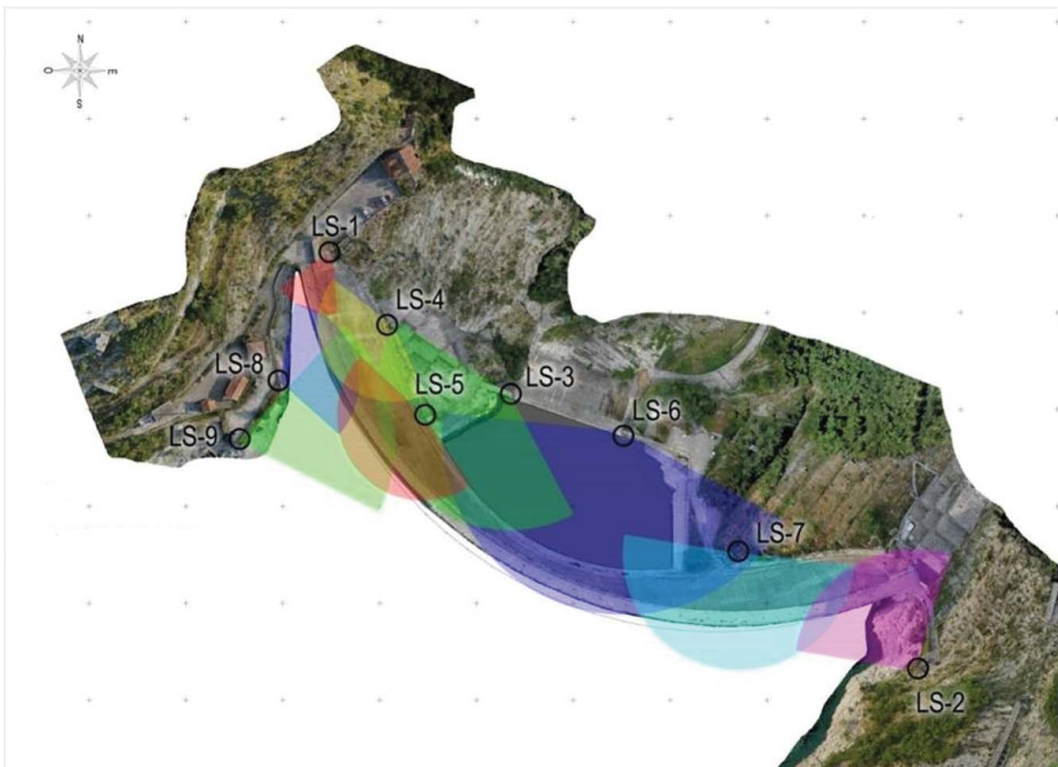
Figure 5. Laser scanner acquisition points and corresponding analysed areas.

Table 2. Laser scanner scans information and comparison with total station data: number of points recorded in each scan (N_p), number of markers used to geo-reference the scans (N_{gm}), differences between target coordinates acquired by total station and laser scanner in terms of average value, standard deviation (σ), maximum and minimum value of the differences along the three components (i.e. east (E), north (N) and altitude (A)).

Laser scanning	N_p (Ml)	N_{gm}	Differences							
			Average value (cm)	σ (cm)	ΔE max (cm)	ΔN max (cm)	ΔA max (cm)	ΔE min (cm)	ΔN min (cm)	ΔA min (cm)
LS-1	16	4	0.5	0.2	0.2	0.2	0.5	−0.3	−0.5	−0.3
LS-2	192	7	0.9	0.3	0.4	1.1	0.7	−0.8	−0.5	−0.8
LS-3	268	23	0.8	0.4	1.1	1.3	1.0	−0.8	−1.0	−1.4
LS-4	340	7	0.9	0.4	1.1	1.0	1.3	−1.4	−0.8	−0.4
LS-5	392	6	0.9	0.4	0.6	1.2	0.5	−0.8	−0.6	−0.9
LS-6	256	25	0.8	0.4	1.2	1.4	1.0	−1.0	−1.0	−1.1
LS-7	320	5	0.7	0.5	1.4	0.6	0.2	−0.5	−0.6	−0.3
LS-8	208	7	0.5	0.2	0.6	0.6	0.3	−0.5	−0.6	−0.4
LS-9	124	4	0.9	0.2	0.8	0.7	0.7	0.4	−0.2	−0.7

be taken as reference scans. Furthermore, Table 2 shows that the maximum and minimum differences are less than 15 mm in the three components of E, N and H. As a result, it is possible to attribute an overall accuracy to the laser scanner model of approximately 15 mm in the three components E, N and H.

Data validation

The validation of the data acquired by the UAV was conducted in several phases, and takes as reference the coordinates of markers and natural points acquired by TS and scans acquired by laser scanner. These measures are more precise than those of the UAV survey. Therefore, the TS and laser scanner data-sets are suitable for the verification of the UAV data surveying. The analysis concerned the evaluation of spatial density, the correspondence of specific points, and linear and surfaces comparisons. In the following subsection, the dense point cloud validation is presented, and an evaluation for density, points, lines and surfaces is performed.

Dense point cloud spatial density validation

The first analysis of the dense point cloud obtained from the acquisition made by UAV is an evaluation of the spatial distribution of the UAV cloud points. We split the dense point cloud into 13 portions to manage the huge amount of data: (1) Downstream face, (2) picnic area, (3) left side, (4) crest, (5) guard house, (6) upstream face first level, (7) galleries, (8) right side, (9) downstream right face, (10) Pulvino (saddle foundation), (12) stilling basin and (13) upstream face second level. The spatial density of points is almost uniform, as can be appreciated from Figure 6, and estimated at a grid 1 cm × 1 cm in size.

Each block, in which the point cloud has been divided, is used for the construction of the point density map. The minimum density is one point every 9 cm^2 (grid 3 cm × 3 cm in size), with a mean value of a one point every 1 cm^2 (grid 1 cm × 1 cm in size). Figures 7 and 8 present the density point maps of some blocks. The lower density is obtained in the areas covered by vegetation, while structural concrete elements are characterized by the highest concentration of points. Table 3 illustrates in detail the number of points and the information related to the density of each analysed block. The dense point cloud has subsequently been purified, in a semi-automatic way, from the main outliers. The UAV dense point cloud is the highest resolution information and it has to be used as a reference and as a starting point for all subsequent processing. The mesh generation from the dense point cloud determines a drastic under sampling of the points with a consequent loss of information. Thus, the metric use of the mesh is to be avoided and all the operations of extraction
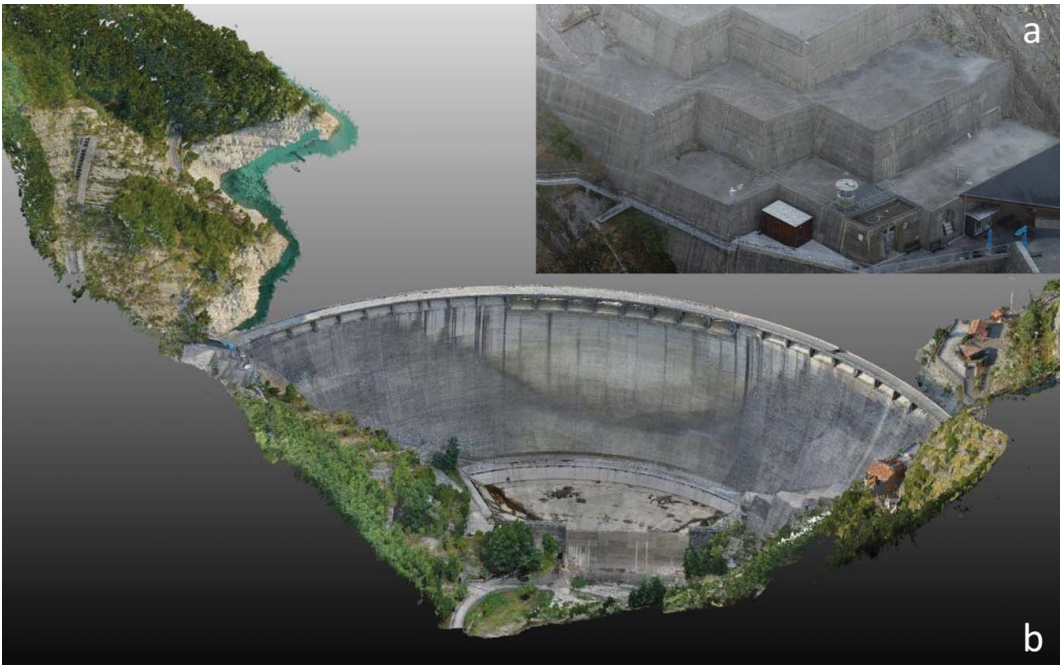
Figure 6. (a) Dense point cloud of the concrete blocks on the right side obtained from UAV – unmanned aerial vehicle – acquisition; (b) Dense point cloud of the whole dam system obtained from UAV – unmanned aerial vehicle – acquisition.
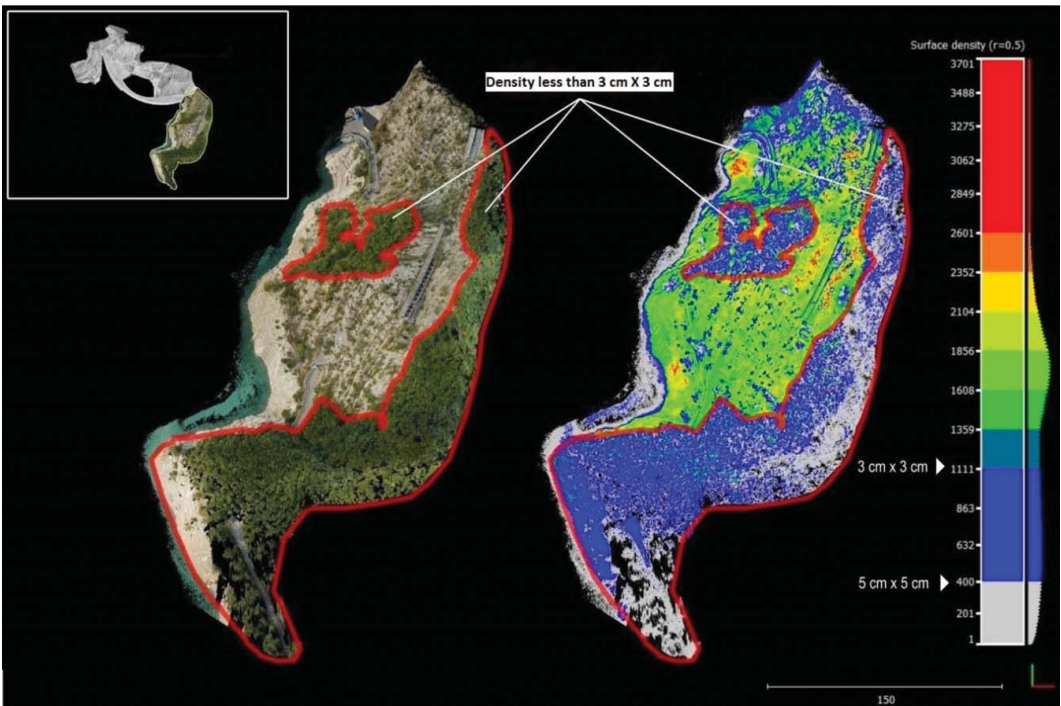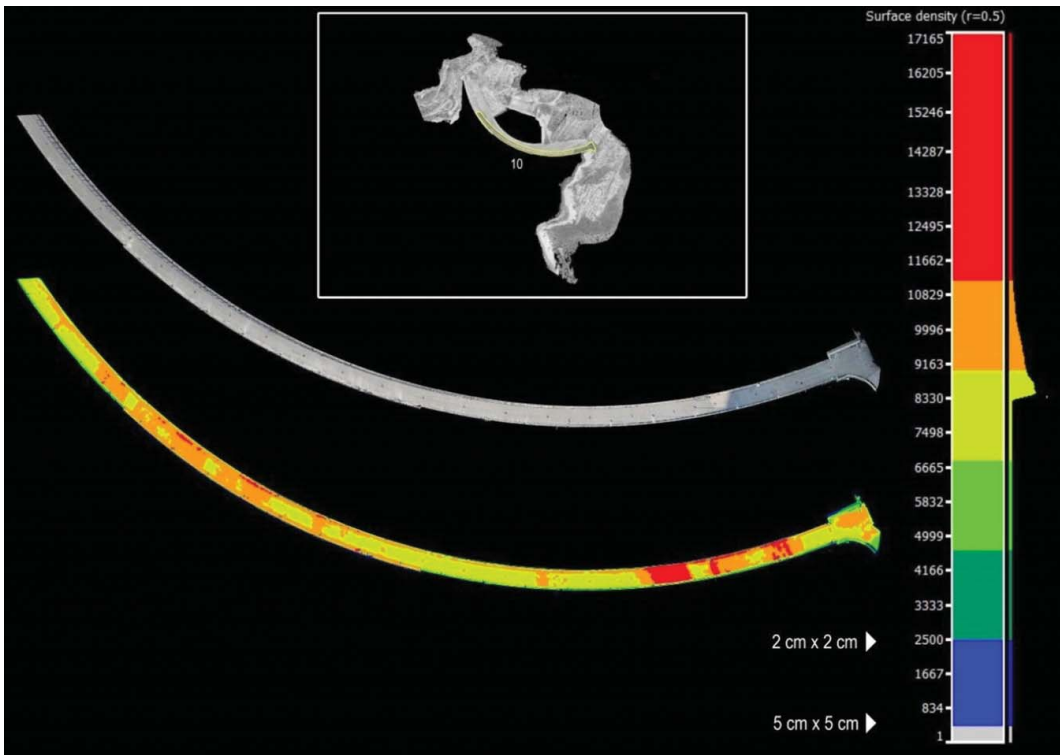

Figure 7. Points density analysis of Block 7, this is an area covered by vegetation and here the points density is lower than in other parts such as the structural parts. The points density is lower than a grid 3 × 3 cm in size.

Figure 8. Points density analysis of Block 10. In this case, the points density is around a grid 1 × 1 cm in size. Structural parts have a higher points density than those covered by vegetation.

of the vertical sections, of the level curves and the of solid structure reconstruction were achieved starting from the base data of dense point cloud.

UAV dense point cloud validation by total station surveying points

The control of points consists in comparing the coordinates of significant points (markers and natural points) acquired by TS and those corresponding to the points of the dense point cloud generated by photogrammetry. A total of 218 points are analysed, of which 146 GCPs, 10 CP – control points and 62 natural points, in accordance with the distribution shown in Figure 9. The analysis of the residues (Table 4) shows that all points have a low mean value and a low standard deviation, thus the

Table 3. Density of the different dense point cloud blocks in points/m² and in grid dimensions.

Block	Medium density (points/m²)	Grid dimension (cm X cm)
1	12,904	1 × 1
2	4030	2 × 2
3	2155	2 × 2
4	28,662	1 × 1
5	1357	3 × 3
6	27,511	1 × 1
7	1244	3 × 3
8	5745	1 × 1
9	6793	1 × 1
10	8827	1 × 1
11	2993	2 × 2
12	7243	1 × 1
13	6736	1 × 1
Average	8938	1 × 1

Figure 9. Planimetry of the acquired points (acquired points and laser scanner acquisition bases).

entire model has the same level of accuracy. The substantial uniformity of the generated global model is demonstrated by the homogeneity of the average values and standard deviations of the different types of points analysed with respect to the three components east (*E*), north (*N*) and altitude (*A*).

UAV dense point cloud validation by laser scanner lines

The verification for lines consists in the comparison between the horizontal sections (contour lines) extracted from the point cloud measured by laser scanner and those obtained by UAV. In this comparison, the laser scanner point cloud is taken as 'Reference' while dense point cloud from UAV as 'Compared.' Nine contour lines are taken into account with a distance of 10 meters (A_{min} = 478 m a.s.l. e A_{max} = 558 m a.s.l.), (Figure 10). The thickness of the slices of points extracted is equal to 3 cm, the set value as a function of the average points density, corresponding to 1 point every 9 cm^2 (a grid 3 cm x 3 cm in size) (Figure 11(a)).

Table 4. Coordinate residuals of the analysed points, markers (GCP – ground control points and CP – control points) and natural points in terms of average vales, standard deviations and minimum and maximum values.

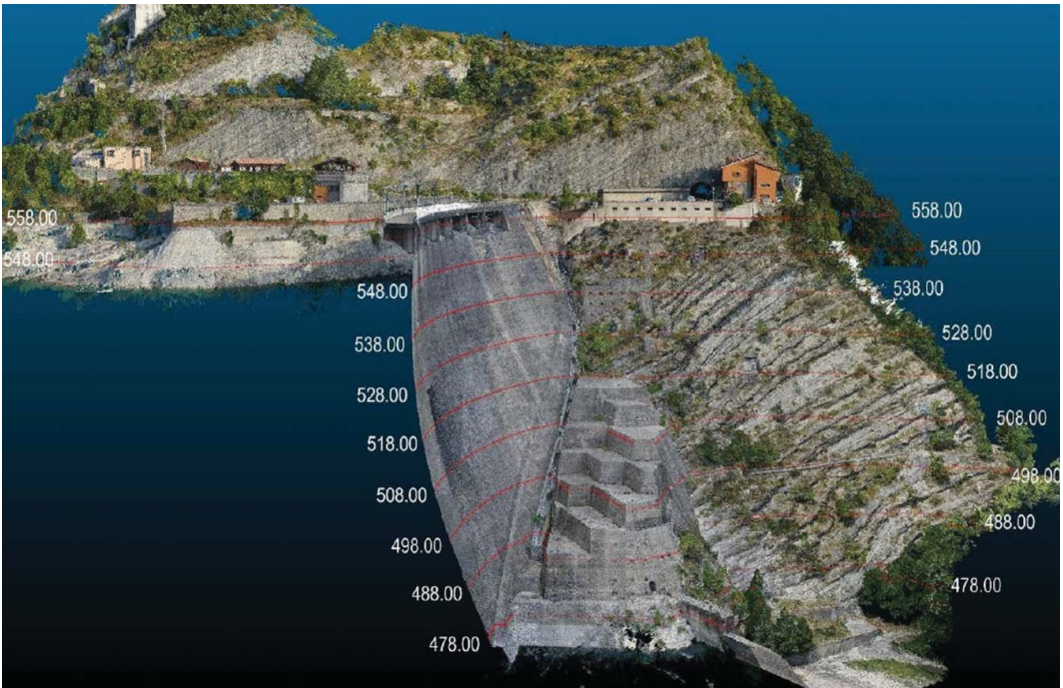|	Markers						Natural points (62)		
	GCP (146)			CP (10)					
	ΔE (cm)	ΔN (cm)	ΔA (cm)	ΔE (cm)	ΔN (cm)	ΔA (cm)	ΔE (cm)	ΔN (cm)	ΔA (cm)
Average	1.0	0.0	0.0	−1.0	1.0	0.0	0.0	0.0	0.0
Standard deviation	2.0	2.0	2.0	2.0	2.0	1.0	3.0	3.0	2.0
Min	−9.0	−6.0	−6.0	−4.0	−1.0	−1.0	−6.0	−10.0	−8.0
Max	8.0	5.0	5.0	2.0	5.0	1.0	6.0	7.0	6.0

Figure 10. Analysed horizontal section on the UAV dense point cloud.

The accuracy of the contour lines is in accordance with those assigned to the laser scanner survey and previously quantified at about 1.5 cm. In almost all cases, the measured points are in a 1.5 cm slice of the polyline automatically generated from the laser scanner points (Figure 11(a)). This characteristic is found on the whole extension of the extracted contour lines, and therefore they are suitable to act as a 'Reference' for the validation of the corresponding curves extracted from the dense point cloud by UAV. Nine horizontal sections are then extracted from the UAV dense point cloud
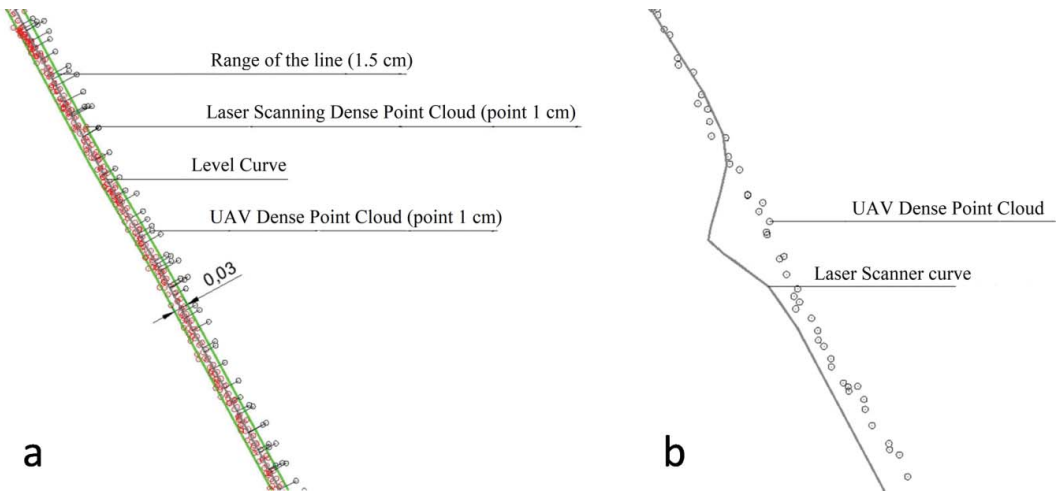

Figure 11. (a) Overlap dense point cloud by laser scanner (points between the range line) and by UAV (points outside the range line). The level curve that interpolates the laser scanner points and the 3 cm laser scanner gap are also reported; (b) Comparison between laser scanner and UAV level curves, near rapid curvature changes the UAV technique cannot recognize the variation.
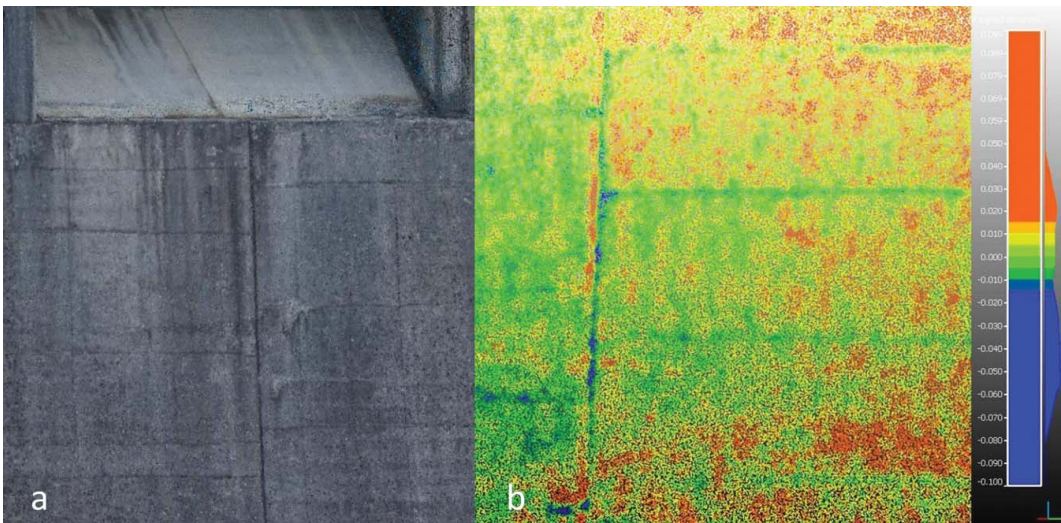
Figure 12. (a) UAV dense point cloud. A small variation such as joints can be recognized by the RGB information associated with the points; (b) Comparison between laser scanner mesh and UAV dense point cloud of a rapid curvature change of the structure, such as joint zones. In this case, the differences between the two entities are at a maximum.
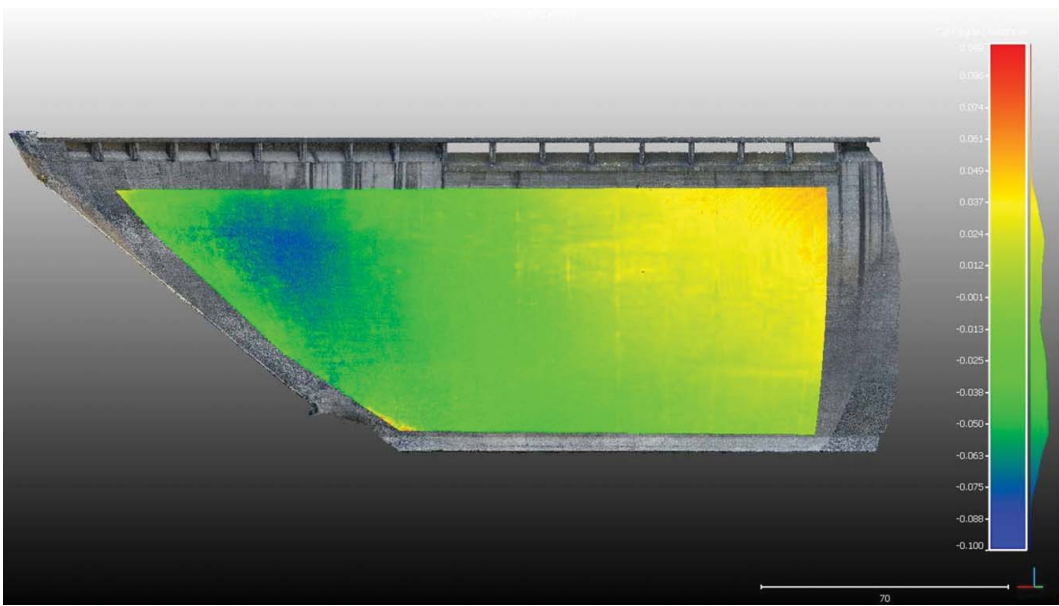
at the same height of those extracted by laser scanner survey. A visual analysis shows how the UAV survey data are characterized by a greater dispersion, especially near fast bend changes (Figure 11 (b)). The joints of the structure are not easily detectable by extracting horizontal sections, but they can be characterized by the analysis of the RGB information of the dense point cloud, as shown in Figure 12(a). The quantitative analysis focuses on the evaluation of the distance between the points that compose the UAV level curves and the polylines extracted from the laser scanner survey employed as 'Reference'. The results are summarized in Table 5. The average distance is of the same order of magnitude as that which characterizes the accuracy of the polylines in the laser scanner survey, which acts as 'Reference'. A wider gap is only reached at the spillway level where the geometry of the structure is very complex.

UAV dense point cloud validation by laser scanner surveying surfaces

The third control phase covers the comparison between laser scanner surfaces and the UAV dense point cloud. This topic is extensively treated, and significant examples that validate the entire model are analysed (Buffi et al. 2016). Therefore, the laser scanner surveying is employed as the 'Reference' of the 'Compared' UAV model. For each analysed specimen, the creation of the 'difference map', as well as the distribution histograms, showing the differences between the laser scanner surfaces and

Table 5. Comparison between UAV points slices and laser scanner curves at the same level, the medium distance between the UAV points and the laser scanner curves is of the same order of magnitude as the standard deviation of the TLS curves.

Curves	Altitude curves (m a.s.l.)	N° points	Medium distance TLS – UAV curves (cm)	Standard deviation TLS curves (cm)
1	558	6680	4.0	3.5
2	548	10,816	2.0	1.7
3	538	16,091	2.0	1.4
4	528	11,313	1.0	10
5	518	12,026	1.0	1.0
6	508	12,181	1.0	1.0
7	498	15,306	1.0	1.3
8	488	7513	2.0	1.7
9	478	3680	3.0	2.0

Figure 13. Surface comparison between laser scanner mesh and UAV dense point cloud of an extended portion on the downstream face. In this case, the differences between the two entities are minimal.

the point clouds, are computed. The deviations, the averages and the standard deviations of the measures are calculated. The specimens taken into account are representative of extended surfaces, changes of curvature and inclined surfaces. At first, the construction of the surface, that interpolates the laser scanner points, and the evaluation of its distance by the same points were performed. The accuracy of the point cloud generated by the laser scanner is, as previously mentioned, about 1.5 cm, while the average deviation and standard deviations of the points from the surfaces generated by them are close to zero, therefore a precision of 1.5 cm can also be considered for them. The accuracy of the mesh from laser scanner makes them suitable as 'Reference' for the UAV surveying. Subsequently, the evaluation of the deviations has been made between the mesh generated by laser scanners and the points of dense point cloud from UAV. A specimen (Figure 13) characterized by a high extension equal to approximately 68% of the total area presents the mean value of the deviations between points and reference mesh equal to −2.1 cm and the standard deviation equal to 3.2 cm. Other specimens (Figure 12(b)) near fast bend changes or joints of the structure, highlight the main difficulty of the UAV survey to capture roughness or indentations of small entities although this may still be possible thanks to RGB information contained in the dense point cloud.

Results

This section summarizes the results of the density, punctual, liner and surface analysis carried out on the UAV dense point cloud. The evaluation of the spatial density on different specimens shows that the density of structure points is never less a point every 9 cm^2 (a grid of 3 × 3 cm in size). Higher densities, around a point every 1 cm^2, are reached on the concrete structure on areas such as the upstream and downstream faces, the crowing and close to the saddle foundation, that are the focus of the survey procedure. Lower density values are reached near areas of vegetation, mostly on the left side, but they are not of interest for the inspection or the geometry reconstruction of the dam. This type of analysis also shows the high uniformity of the UAV data. Therefore, thanks also to the RGB information associated to the points, it allows a detailed inspection of the concrete surface.

The validation by point consists in the evaluation of the distance between two sets of data: the reference markers acquired by TS (i.e. control points) and the same generated by the UAV dense point cloud. The gap of a few centimetres and the global uniformity of the UAV model are ensured by the average values and homogeneity of the standard deviations of the analysed points along the three components. The validation by lines evaluates the distance between nine curves extracted, respectively, by the laser scanner model and by the UAV dense point cloud at the same level. The average value of the gap is 2 cm, the maximum distance is evaluated near the higher level curves (558 m a.s.l.), where the geometry of the structure is very complex due to the presence of the lights of the spillways. Moreover, in this area there is the combination of air updrafts, due to the temperature difference between the bottom and the top of the structure, and the air flowing from the spillways lights. Therefore, the UAV was unable to fly, for safety reasons, close to the structure.

Finally, the validation by surfaces evaluates the distance between the mesh built on the laser scanner scans and the UAV dense point cloud. Also in this case, different specimens are taken into account. A uniform surface such as that of the downstream facing dam shows a mean value of the gap of 2.1 cm. Other parts of the structure, such as those characterized by rapid curvature change in a small space such as joints and spillways lights, show higher distances. To reduce the gaps, some markers could be placed close to the curvature changes fixing the model exactly in its most critical points. However, small variations in the geometry are in any case detectable by the RGB information associated with the UAV dense point cloud.

Conclusions and future developments

The application of UAV to infrastructure surveys with a complex geometrical shape, such as dams is the basis, when adequately supported by topographic instruments, for the development of an accurate metric reconstruction. The work presents an operative procedure for UAV surveying and the dense point cloud validation of masonry dams applied to a concrete arch gravity dam located in central Italy: the Ridracoli dam.

The drone technique makes it possible to cover, with more than 3000 frames, the entire dam system; the correct geo-referencing and matching of the dense point cloud is ensured by the placement and acquisition of the coordinates, also using traditional topographic tools (i.e. TS, laser scanner and GPS Station), of 218 points, between markers and natural points. The placement of the markers and the choice of the natural points have to be accurate. They have to be well spaced and uniformly placed on the object of the survey to avoid local distortions and to reduce the global error of the dense point clouds especially close to the boundaries. A study on the correct configuration in terms of numbers and disposition of markers on vertical structure will follow the present work. The efficiency and effectiveness of the UAV techniques is evidenced by its rapidity and economy (acquisition phase) and by punctual, linear and surface data accuracy (processing phase).The potential deployment and future developments of the UAV product are various.

Some areas of the Ridracoli dam and similar, because of their reduced accessibility, would require considerable safety inspections work (involving climbers) and the simultaneous sharing of information among maintenance and management technicians would not always be possible. Furthermore, the possibility to have a photographic record of every detail of the structure allows for shared participation and establishes a base level by which to monitor the evolution of the structure conservation status so that would be possible to pass from a 'run to failure' maintenance management to a predictive and proactive one. And over the traditional methods, often, appear complex and not exhaustive. This problem, with this experience, seems to be passed by using an innovative UAV. The speedy flight and its repeatability give us the possibility to forecast a rapid ageing so to prevent a partial loss of safety with sustainable costs. The elimination of these inefficiencies can lead through effective maintenance practices, and can reduce costs between 40% and 60%.

The validated dense point cloud model constitutes the basis for the development of a 3D model for FE analyses. The possibility to schematize structurally significant elements such as construction

joints and spillways or accessory elements of the dam body, such as the stilling basin and weight blocks in the sides, allows the simulation of the correct loads and deformability conditions of the surrounding lands. The modelling of the morphology of the surrounding land is a further development of the model simulating the current condition of the structure constraint. The subdivision of the structure into independent solid elements enables the application of mechanical properties of materials, of different boundary conditions and of different interaction conditions. Indeed, the high level of detail of the UAV survey allows the modelling of the transition surfaces between different structural elements or ancillary works and the surrounding soil. Static and dynamic analysis, following the application of cause quantities such as the hydrostatic level, temperature and seismic accelerations, allow the evaluation of stress and strain states, in particular near discontinuous surfaces such as the joints of the structure. Therefore, the dense point cloud model is the first step towards building a realistic 3D FEM (finite element method) model, through which it is possible to simulate scenarios that have affected, or could affect, the structure. It could also be a useful cognitive instrument to simulate the evolution of the mechanical properties of the structure.

Acknowledgments

Disclosure statement

No potential conflict of interest was reported by the authors.

Funding

ORCID

Giulia Buffi 🆔 http://orcid.org/0000-0001-7624-1642

References

Achille C, Adami A, Chiarini S, Cremonesi S, Fassi F, Fregonese L, Taffurelli L. 2015. UAV-based photogrammetry and integrated technologies for architectural applications — methodological strategies for the after-quake survey of vertical structures in Mantua (Italy). Sensors. 15(7):15520–15539.

Alfonso L, Ridolfi E, Gaitan S, Napolitano F, Russo F. 2014. Ensemble entropy for monitoring network design. Entropy. 16(3):1365–1375.

Alpina S.p.A., Consorzio Acque Forlì Ravenna. 1985. Diga di Ridracoli.

Amorocho J, Espildora B. 1973. Entropy in the assessment of uncertainty in hydrologic systems and models. Water Resour Res. 9:1511–1522.

Andrews DP, Bedford J, Bryan PG. 2013. A comparison of laser scanning and structure from motion as applied to the great barn at Harmondsworth, UK. International archives of the photogrammetry, remote sensing and spatial information sciences. Volume XL-5/W2, 2013XXIV. Proceedings of the International CIPA Symposium; Sep 2–6; Strasbourg.

Barry P, Coakley R. 2013. Field accuracy test of RPAS photogrammetry. Int Arch Photogramm Remote Sens Spatial Inf Sci. 40(1):27–31.

Biscarini C, Di Francesco S, Manciola P. 2010. CFD modelling approach for dam break flow studies. Hydrol Earth Syst Sci. 14(4):705–718.

Biscarini C, Di Francesco S, Nardi F, Manciola P. 2013. Detailed simulation of complex hydraulic problems with macroscopic and mesoscopic mathematical methods. Math Prob Eng. 2013:1–14.

Biscarini C, Di Francesco S, Ridolfi E, Manciola P. 2016. On the simulation of floods in a narrow bending valley: the Malpasset Dam Break case study. Water. 8(11):1–19.

Bolognesi M, Furini A, Russo V, Pellegrinelli A, Russo P. 2014. Accuracy of cultural heritage 3D models by RPAS and terrestrial photogrammetry. Int Arch Photogramm Remote Sens Spatial Inf Sci. XL-5:113–119.

Bolognesi M, Furini A, Russo V, Pellegrinelli A, Russo P. 2015. Testing the low-cost RPAS potential in 3D cultural heritage reconstruction. Int Arch Photogramm Remote Sens Spatial Inf Sci. XL-5/W4:229–235.

Buffi G, Grassi S, Manciola P, Niemeier W. 2016. Comparison of 3D model derived from UAV and TLS – The experience at Ridracoli Dam, Italy. Terrestrisches Laserscanning 2016 (TLS). Proceedings of Terrestrisches Laserscanning 2016; Nov 28–29; Fulda.

Casadei S, Manciola P. 1995. Criteria for the evaluation of the rate of water use in a river basin. IAHS. 231:169–179.

Colomina I, Molina P. 2014. Unmanned aerial systems for photogrammetry and remote sensing: a review. ISPRS J Photogramm Remote Sens. 92:79–97.

Consorzio Acque per le Province di Forlì e Cesena. 1991. L'acquedotto della Romagna [Aqueduct of Romagna].

DM Infrastrutture 14 gennaio 2008. Nuove Norme Tecniche per le costruzioni [New Technical Regulations for the Constructions(Italy)].

Dominici D, Alicandro M, Massimi V. 2016. UAV photogrammetry in the post-earthquake scenario: case studies in L'Aquila. Geomat Nat Haz Risk. 8:1–4.

Ellenberg A, Branco L, Krick A, Bartoli I, Kontsos A. 2014. Use of unmanned aerial vehicle for quantitative infrastructure evaluation. J Infrastruct Syst. 3:04014054.

Ellenberg A, Kontsos A, Bartoli I, Pradhan A. 2014. Masonry crack detection application of an unmanned aerial vehicle. Proceedings in the International Conference on Computing in Civil and Building Engineering 2014. p. 1788–1795.

Froelich DC. 2008. Embankment Dam breach parameters and their uncertainties. J Hydraul Eng. 134(12):1708–1721.

Gillins M, Gillins D, Parrish C. 2016. Cost-effective bridge safety inspections using unmanned aircraft systems (UAS). Geotechnical and Structural Engineering Congress 2016; Feb 14–17; Phoenix, AZ. p. 1931–1940.

Gonçalvesa JA, Henriques R. 2015. UAV photogrammetry for topographic monitoring of coastal areas. ISPRS J Photogramm Remote Sens. 104:101–111.

Hallermann N, Morgenthal G. 2016. From aerial photography to 3-dimensional inspection of bridges. Proceedings in the IABSE Conference 2016; May 8–11; Guangzhou.

Hallermann N, Morgenthal G, Rodehorst V. 2014. Vision-based deformation monitoring of large scale structures using Unmanned Aerial Systems. IABSE Symposium Report. 102(8):2852–2859.

Hallermann N, Morgenthal G, Rodehorst V. 2015. Unmanned Aerial Systems (UAS) – Survey and monitoring based on high-quality airborne photos. Proceedings in the IABSE Conference; Sep 23–25; Geneva.

[ICOLD] International Commission on Large Dams. 2016. Role of dams; [accessed 2016 Dec 21]. http://www.icold-cigb.net/GB/Dams/role_of_dams.asp.

[INGV] National Institute of Geophysics and Volcanology. 2016. [accessed 2016 Nov 15]. http://www.pi.ingv.it/banche-dati/.

Irschara A, Zach C, Frahm JM, Bischof H. 2009. From structure-from-motion point clouds to fast location recognition. Proceedings of the IEEE Conference on Computer Vision and Pattern Recognition; Jun 20–25; Miami, FL.

Kim B, Sanders BF. 2016. Dam-break flood model uncertainty assessment: case study of extreme flooding with multiple dam failures in Gangneung, South Korea. J Hydraul Eng. 142(2):05016002.

Mancini F, Dubbini M, Gattelli M, Stecchi F, Fabbri S, Gabbianelli G. 2013. Using Unmanned Aerial Vehicles (UAV) for high-resolution reconstruction of topography: The structure from motion approach on coastal environments. Remote Sens. 5(12):6880–6898.

Marcello A, Fornari F. 2012. GdL Riabilitazione delle dighe in Italia - RAPPORTO FINALE [Group of work, Riabilitation of dams in Italy]. ITCOLD.

Naumann M, Geist M, Bill R, Niemeyer F, Grenzdörffer G. 2013. Accuracy comparison of digital surface models created by unmanned aerial systems imagery and terrestial laser scanner. Remote SensSpatial Inf Sci. XL-1/W2:1–13.

Olsen NRB, Kjellesvig HM. 2010. Three-dimensional numerical flow modelling for estimation of spillway capacity. J Hydraul Res. 141:775–784.

Ouédraogo MM, Degré A, Debouche C, Lisein J. 2014. The evaluation of unmanned aerial system-based photogrammetry and terrestrial laser scanning to generate DEMs of agricultural watersheds. Geomorphology. 214:339–355. Elservier.

Püschel H, Sauerbier M, Eisenbeiss H. 2008. A 3D model of Castle Landemberg (CH) from comc UAV-based images. Remote Sens Spatial Inf Sci. 96–98.

Ridolfi E, Alfonso L, Di Baldassarre G, Dottori F, Russo F, Napolitano F. 2014. An entropy approach for the optimization of cross-section spacing for river modeling. Hydrol Sci J. 59(1):126–137.

Ridolfi E, Buffi G, Venturi S, Manciola P. 2017. Accuracy analysis of a dam model from drone surveys. Sensors. 17:1777.

Ridolfi E, Yan K, Alfonso L, Di Baldassarre G, Napolitano F, Russo F, Bates PD. 2012. An entropy method for flood-plain monitoring network design. Proceedings in the AIP Conference; Sep 5–8, 2011; Gdańsk, Poland. p. 1780.

Salvini R, Mastrorocco G, Seddaiu M, Rossi D, Vanneschi C. 2016. The use of an unmanned aerial vehicle for fracture mapping within a marble quarry (Carrara, Italy): photogrammetry and discrete fracture network modeling. Geomat Nat Haz Risk. 8:34–52.

Shannon CE. 1948. A mathematical theory of communication. Bell SystTech J. 27:379–423.

Skarlatos D, Procopiou E, Stavrou G, Gregoriou M. 2013. Accuracy assessment of minimum control points for UAV photography and georeferencing. Proceedings in the First International Conference on Remote Sensing and Geo-information of the Environment; Apr 8–10; Cyprus.

Tahar KN. 2013. An evaluation on different number of ground control points in unmanned aerial vehicle photogram-metric block. In International Archives of the Photogrammetry. Remote Sensing and Spatial Information Sciences. Xl-2/W2:93–98.

Tang WH, Yen BC. 1991. Dam safety inspection scheduling, JHydraul Eng. 117(2):93–98.

Teza G, Pesci A, Ninfo A. 2016. Morphological analysis for architectural applications: Comparison between laser scanning and structure-from-motion photogrammetry. J Surv Eng. 142(3):04016004.

Tortajada C. 2014. Dams: an essential component of development. J Hydrol Eng. 20:A4014005-1–A4014005-9.

Turner D, Lucieer A, Watson C. 2012. An automated technique for generating georectified mosaics from ultra-high resolution unmanned aerial vehicle (UAV) imagery, based on structure from motion (SfM) point clouds. Remote Sens. 4(5):1392–1410.

Ullman S. 1979. The interpretation of structure from motion, Proc Royal Soc B: Biol Sci. 203:405–426.

Venturi S, Di Francesco S, Materazzi F, Manciola P. 2016. Unmanned aerial vehicles and geographical information system integrated analysis of vegetation in Trasimeno Lake, Italy. Lakes Reserv Res Manage. 21:5–19.

Vetrivel A, Gerke M, Kerle N, Vosselman G. 2015. Identification of damage in buildings based on gaps in 3D point clouds from very high resolution oblique airborne images. ISPRS J Photogrammet Remote Sens. 105:61–78.

Wuajanz D, Holst C, Neitzel F, Kuhlmann H, Niemeier W, Schwieger V. 2016. Survey configuration for terrestrial laser scanning. Allgemeine Vermessungs-Nachrichten (AVN). 123:158–169.

Zech Y, Soares-Frazão S. 2007. Dam-break flow experiments and real-case data. A database from the European IMPACT research. J Hydraul Res. 45(sup1):5–7.